

Equilibrium and Aging Dynamics of Simple Models for Glasses

A. Crisanti[†] and F. Ritort[‡]

[†] Dipartimento di Fisica, Università di Roma “La Sapienza” and
Istituto Nazionale Fisica della Materia, Unità di Roma
P.le Aldo Moro 2, I-00185 Roma, Italy

[‡] Physics Department, Faculty of Physics
University of Barcelona, Diagonal 647, 08028 Barcelona, Spain

Abstract. We analyze the properties of the energy landscape of *finite-size* fully connected p -spin-like models. In the thermodynamic limit the high temperature phase is described by the schematic Mode Coupling Theory of super-cooled liquids. In this limit the barriers between different basins are infinite below the critical dynamical temperature the ergodicity is broken on infinite times. We show that *finite-size* fully connected p -spin-like models, where activated processes are possible, do exhibit properties typical of real super-cooled liquid when both are near the critical glass transition. Our results support the conclusion that fully-connected p -spin-like models are the natural statistical mechanical models for studying the glass transition in super-cooled liquids.

PACS numbers: 64.70.Pf, 75.10.Nr, 61.20.Gy, 82.20.Wt

Introduction

In recent years a significant effort has been devoted to understand slow relaxation dynamics observed in many, apparently unrelated, systems such as structural glasses, spin glasses, disordered and granular materials or proteins among others. In such systems the characteristic relaxation time may change of many orders of magnitude if the external parameters, e.g. the temperature T , are slightly varied. As a consequence correlations display non-exponential behavior, and equilibration processes slow down giving rise to non-equilibrium phenomena known as aging.

The common denominator which makes all these systems displaying similar behavior near the (dynamical) critical temperature is the complexity of the energy landscape. The trajectory of the representative point in the configuration space can be viewed as a path in a multidimensional potential energy surface [1]. The dynamics is therefore strongly influenced by the topography of the potential energy landscape: local minima, barriers, basins of attraction and other topological properties all influence the dynamics.

The potential energy surface of a super-cooled liquid contains a large number of local minima, called *inherent structures* (IS) by Stillinger [2]. All states that under local energy minimization will flow into the same IS define the *basin* of the IS (valley). With this picture in mind the time evolution of the system can be seen as the result of two different processes: thermal relaxation into basins (*intra-basin* motion) and thermally activated potential energy barrier crossing between different basins (*inter-basin* motion). When the temperature is lowered down to the order of the critical Mode Coupling Theory (MCT) temperature T_{MCT} the inter-basin motion slows down and the relaxation dynamics is dominated by the slow thermally activated crossing of potential energy barriers [3]. If the temperature is further reduced the relaxation time eventually becomes of the same order of the observation time and the system falls out of equilibrium since there is not enough time to cross barriers and equilibrate. This defines the “experimental” glass transition temperature T_g .

The regime between T_{MCT} and T_g cannot be described by the MCT since it neglects activated processes responsible for barrier crossing. In MCT the relaxation time diverges at T_{MCT} , leading to $T_g = T_{MCT}$, and the dynamics remains confined into a single basin forever. Attempts to overcome these difficulties in MCT have been done, but probably the most clear picture comes from some spin-glass models. The essential features of MCT for glass-forming systems are also common to some fully connected spin glass models [4], the most well known being the spherical p -spin spin glass model [6, 5]. We shall call these models *mean-field p -spin-like* glass models. The central point is that near T_{MCT} the behavior of the system is mainly due to the IS organization (density, basins, barriers and so on), so that all systems with similar IS structure should have similar critical behavior.

In the thermodynamic limit the high-temperature phase – paramagnetic in the spin-glass language and liquid in glass language – of mean-field p -spin-like is described by the schematic MCT for super-cooled liquids [7, 5]. As a consequence at the critical temperature, called T_D in p -spin language, an ergodic to non-ergodic transition takes place. Below this temperature the system is dynamically confined to a metastable state (a basin) [8] since relaxation to true equilibrium can only take place via activated processes, absent in mean-field models. Therefore in mean-field models, similar to what happens in MCT, at T_D the relaxation time diverges. For these systems, nevertheless, it is known that the true equilibrium transition to a low temperature

phase occurs below T_D at the static critical temperature T_c , also denoted by T_{1rsb} [6]. This is the analogous of the Kauzmann temperature T_k for liquids. The glass transition temperature T_g of real systems sits somewhere in between T_c and T_D . This transition, obviously, cannot be reached even on infinite time in mean-field models.

Despite these difficulties mean-field models, having the clear advantage of being analytically tractable, have been largely used to study the properties of fragile glassy systems, especially between the dynamical temperature T_D and the static temperature T_c where a real thermodynamic phase transition driven by the collapse of the configurational entropy takes place. The picture that emerges is however not complete since activated process cannot be captured by mean-field models. Therefore the relevance of mean-field results for real systems it is still not completely stated. Let us also remark that, despite the large amount of analytical work devoted to the study of the static as well as dynamical properties in the $N \rightarrow \infty$ limit, much less is known concerning the finite N behavior.

In this work we investigate numerically *finite-size* fully-connected p -spin-like models, where activated processes *are* present. Comparing our results with the observed behavior of super-cooled liquids near T_{MCT} we conclude that, once activated process are allowed, mean-field p -spin-like models are highly valuable for a deep understanding of the glass transition in real systems.

All results reported here are for the Ising-spin Random Orthogonal Model (ROM) [10, 11], however similar results are obtained using other p -spin-like models, as for example the Bernasconi Model and the Ising p -spin model. The advantage of ROM lies in its interaction term which is two-body, at difference with the p -body interaction of p -spin models, reducing computer memory problems. Moreover the use of Ising spins instead of continuous spins, as for the spherical p -spin model, allows for a larger configuration entropy and faster algorithms. Preliminary results for the spherical p -spin model are in qualitative agreement with those reported here.

1. Thermodynamics of Inherent Structures: How to evaluate the configurational entropy

The Random Orthogonal Model model is defined by the Hamiltonian [10, 11],

$$H = -2 \sum_{ij} J_{ij} \sigma_i \sigma_j \quad (1)$$

where $\sigma_i = \pm 1$ are N Ising spin variables, and J_{ij} is a $N \times N$ random symmetric orthogonal matrix with $J_{ii} = 0$. Numerical simulations are performed using the Monte Carlo method with the Glauber algorithm. For $N \rightarrow \infty$ this model has the same thermodynamic properties of the p -spin model: a dynamical transition at $T_D = 0.536$, with threshold energy per spin $e_{th} = E_{th}/N = -1.87$, and a static transition at $T_c = 0.25$, with critical energy per spin $e_{1rsb} = -1.936$ [10, 11].

The TAP analysis [8, 11] reveals that the phase space visited is composed by an exponentially large (in N) number of different basins, each labelled by the value of the energy density e at $T = 0$, separated by infinitely large (for $N \rightarrow \infty$) barriers. The free energy of the e -TAP solution describes the thermodynamics within the basins labelled by e and at $T = 0$ coincides with the local minima potential energy, i.e., the IS of the system. The dynamical transition is associated with IS having the largest basin of attraction for $N \rightarrow \infty$, while the static transition with IS having the lowest accessible free energy [8, 12].

In the mean-field limit, the allowed values of e are between e_{1rsb} and e_{th} . Solutions with e larger than e_{th} are unstable (saddles), while solutions with e smaller than e_{1rsb} have negligible statistical weight. Moreover in the $N \rightarrow \infty$ limit IS with $e = e_{th}$ attract most (exponentially in N) of the states and dominate the behavior of the system. Other IS are irrelevant for $N \rightarrow \infty$.

For finite N the scenario is different since not only the basins of IS with $e < e_{th}$ acquire statistical weight, but it may happen that solutions with $e > e_{th}$ and few negative directions (saddles with few downhill directions) become stable, simply because there are not enough degrees of freedom to hit them.

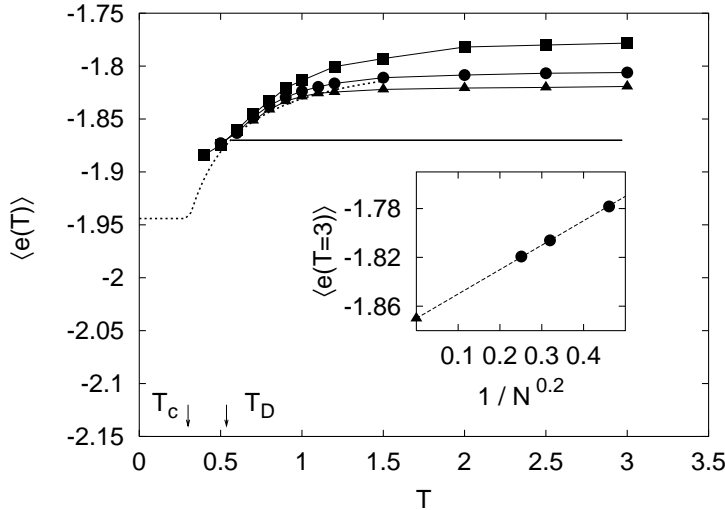


Figure 1. Temperature dependence of $\langle e(T) \rangle$ for $N = 48$ (square), $N = 300$ (circle) and $N = 1000$ (triangle). The average is over 10^3 different equilibrium configurations at temperature T . The horizontal line is the $N \rightarrow \infty$ limit. The arrows indicate the critical temperatures T_D and T_c (see text). The dotted line is the curve obtained from the configurational entropy for large N . Inset: size dependence of $\langle e(T=3) \rangle$ as a function $N^{-\alpha}$ with $\alpha = 0.2$ extrapolated down to the $N \rightarrow \infty$ theoretical result -1.87 (triangle).

To get more insight the IS-structure of finite systems we follow Stillinger and Weber [13] and decompose the partition sum into a sum over basins of different IS and a sum within each basin. Collecting all IS with the same energy e , denoting with $\exp[Ns_c(E)] de$ the number of IS with energy between e and $e + de$, and shifting the energy of each basin with that of the associated IS, the partition sum can be rewritten as [13]

$$Z_N(T) \simeq \int de \exp N [-\beta e + s_c(e) - \beta f(\beta, e)] \quad (2)$$

where $f(\beta, e)$ can be seen as the free energy density of the system when confined in one of the basin associated with IS of energy e . The function $s_c(e)$ is the *configurational entropy density* also called *complexity*. From eq. (2) we easily obtain the probability that an equilibrium configuration at temperature $T = 1/\beta$ lies in a basin associated with IS of energy between e and $e + de$:

$$P_N(e, T) = \exp N [-\beta e + s_c(e) - \beta f(\beta, e)] / Z_N(T). \quad (3)$$

Taking the $N \rightarrow \infty$ limit we recover the mean-field results [8, 10, 11].

From the partition function (2) we can easily compute the average internal energy density given by $u(T) = \langle e + \partial(\beta f)/\partial\beta \rangle = \langle e(T) \rangle + \langle \Delta e(T) \rangle$. The first term is the average energy of the IS relevant for the thermodynamics at temperature T , while the second term is the contribution from fluctuations inside the basin of the IS. The average is taken with the weight (3).

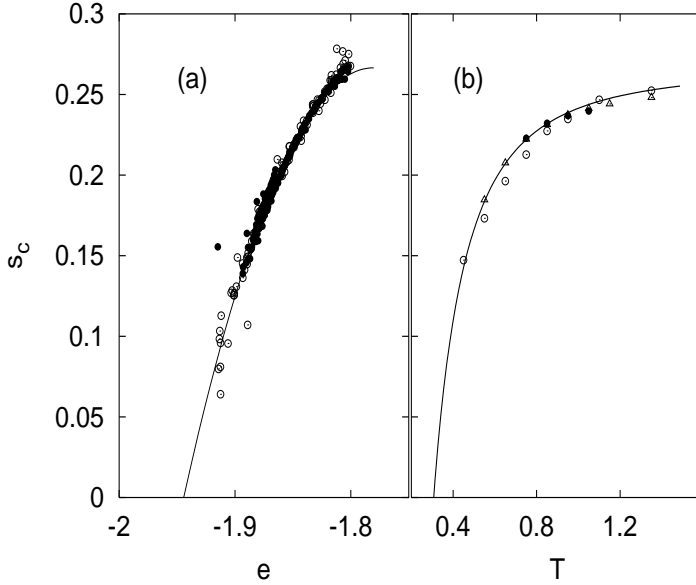


Figure 2. (a) Configurational entropy as a function of energy. The data are from system sizes $N = 48$ (empty circle) and $N = 300$ (filled circle), and temperatures $T = 0.4, 0.5, 0.6, 0.7, 0.8, 0.9$ and 1.0 . For each curve the unknown constant has been fixed to maximize the overlap between the data and the theoretical result [11]. The line is the quadratic best-fit. (b) Configurational entropy density as a function of temperature. The line is the result from the best-fit of $s_c(e)$ while the symbols are the results from the temperature integration of eq. (6) for $N = 48$ (empty circle), $N = 300$ (empty triangle) and $N = 1000$ (filled circle).

Since we are interested into the IS structure we shall concentrate on $\langle e(T) \rangle$. In the limit $N \rightarrow \infty$ the only relevant IS are those with $e = e_{th}$, and $\lim_{N \rightarrow \infty} \langle e(T) \rangle = e_{th}$ for any $T > T_D$. To measure $\langle e(T) \rangle$ for finite N we perform the following experiment. First we equilibrate the system at a given temperature T , then starting from an equilibrium configuration we instantaneously quench it down to $T = 0$. This is obtained by decreasing the energy along the steepest descent path. In this way we can identify the energy of the IS visited by the equilibrium trajectory. The experiment is repeated several times starting from uncorrelated equilibrium configurations at T and the average IS energy is computed. In figure 1 we report $\langle e(T) \rangle$ as a function of temperature T for system sizes $N = 48, 300$ and 1000 . As expected, as N increases $\langle e(T) \rangle$ tends towards e_{th} . From the numerical data we found that the plateau energy, approaches e_{th} with the power law $\langle e_{plateau} \rangle - e_{th} \sim N^{-0.2}$, see inset Fig. 1. Note that since N is finite we can equilibrate the system also below T_D , down to the glassy transition $T_g(N)$, about 0.35 for $N = 48$ and 0.5 for $N = 300$, below which the system falls out of equilibrium [14].

The figure shows that for finite N and T not too close to T_D the thermodynamics is dominated by IS with $e > e_{th}$. This is more evident from the (equilibrium) probability distribution of e since it is centered about $\langle e(T) \rangle$ indicating that IS with $e \simeq \langle e(T) \rangle$ have the largest basins. This scenario has been also observed in real glass-forming systems [15, 16, 17, 18, 19].

From the knowledge of IS-energy distribution we can reconstruct the complexity $s_c(e)$. In the temperature range where eq. (3) is valid, we have

$$s_c(e) = \ln P_N(e, T) + \beta e + \beta f(\beta, e) + \ln Z_N(T) \quad (4)$$

If energy dependence of $f(\beta, e)$ can be neglected, then it is possible to superimpose the curves for different temperatures. The resulting curve is, except for an unknown constant, the complexity $s_c(e)$. The curves obtained for system sizes $N = 48$ and 300 and various temperatures between $T = 0.4$ and $T = 1.0$ are shown in figure 2 (a). The data collapse is rather good for $e < -1.8$. Above the curves cannot be superimposed anymore indicating that the energy dependence of $f(\beta, e)$ cannot be neglected. In liquid this is called the anharmonic threshold [20, 21]. To compare the result with the known analytical predictions for the ROM each curve in the figure has been translated to maximize the overlap with the theoretical prediction for $s_c(e)$ [11]. The dotted line is the quadratic best fit from which we can estimate the critical energy $e_c \simeq -1.944$ as the value where $s_c(e)$ vanishes in good agreement with the theoretical result $e_{1rsb} = -1.936$ [11].

Direct consequence of $f(\beta, e) \simeq f(\beta)$ for $e < -1.8$ is that in this range the partition function can be written as the product of an intra-basin [22] contribution [$\exp(-N\beta f)$] and of a configurational contribution which depends only on the IS energy densities distribution. The system can then be considered as composed by two independent subsystems: the intra-basin subsystem describing the equilibrium when confined within basins, and the IS subsystem describing equilibrium via activated processes between different basins. As the temperature is lowered and/or N increased the two processes get more separated in time and the separation into two subsystems becomes more and more accurate. A scenario typical of super-cooled liquids near the MCT transition [23, 3].

The form of $f(\beta)$ for the specific system can be computed studying the motion near the IS, for example using an harmonic approximation [20, 21]. However, this usually gives only a small corrections to thermodynamic quantities for T close to T_D [20, 21] and we do not consider it here.

Another important consequence of the separation into two subsystems is that in eq. (3) $f(\beta, e)$ can be neglected since it cancels with the equal term coming from the denominator. Therefore from the knowledge of $s_c(e)$ we can easily compute the average IS energy density $\langle e(T) \rangle$. For large N this is given by the saddle point estimate, see eq. (3):

$$\max_e [-\beta e + s_c(e)]. \quad (5)$$

The result obtained using for $s_c(e)$ the quadratic best-fit of figure 2 (a) is the dotted line shown in Fig. 1. The agreement with the direct numerical data is good already for $N = 300$. From the form of $\langle e(T) \rangle$ for large N we can identify the static critical temperature $T_c \simeq 0.3$ as the temperature below which $\langle e(T) \rangle$ remains constant, not far from the theoretical results $T_c = 0.25$ [11].

To have a check of our results we have computed the configurational entropy density using a different approach [20]. When the IS subsystem is in thermal

equilibrium then the temperature dependence of the configurational entropy density can be evaluated from the thermodynamic relation

$$\frac{ds_c(T)}{d\langle e(T) \rangle} = \frac{1}{T} \quad (6)$$

integrating the T dependence of $d\langle e(T) \rangle/T$. Using the data of figure 1 we obtain the curves shown in figure 2 (b). The line is the result valid for large N obtained from the quadratic best fit of $s_c(e)$ [figure 2 (a)]. The agreement for $N = 300$ and 1000 is rather good. Note that increasing N reduces the IS energy range explored by the system for a given fixed Montecarlo simulation length. This in turn reduces the temperature range in figure 2 (b).

To have a statistical description of the energy landscape we also investigated cross correlations among IS and equilibrium configurations at T . It emerges that while the equilibrium configuration is highly correlated with the corresponding IS, different IS are uncorrelated. Moreover the probability distribution of IS-IS overlaps is a Gaussian centered in zero and variance which goes to zero as N increases. The analysis of triplet of IS does not reveal any particular organization of states. This result, characteristic of the Random Energy Model [24], is known to hold also for multispin interaction spin-glass models.

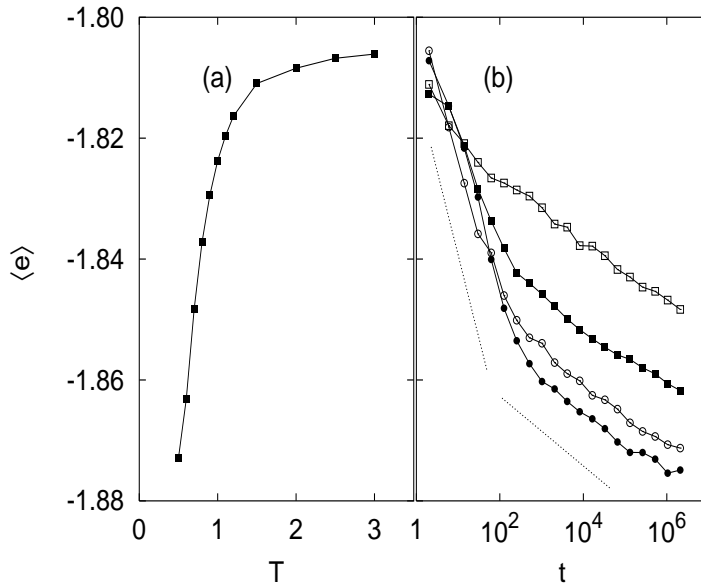


Figure 3. Average inherent structure energy in equilibrium as a function of temperature (a) and as a function of time during the non-equilibrium process (b). The system size is $N = 300$, $T_i = 3.0$ and (top to bottom) $T_f = 0.1, 0.2, 0.3$ and 0.4 (panel b).

2. Non-equilibrium behavior: the role of activated processes

More informations on the IS structure can be obtained from non-equilibrium relaxation processes. To study the non-equilibrium dynamics we quench at time zero the system

from an initial equilibrium configuration at temperature $T_i > T_g$ to a final temperature $T_f < T_g$ and study the evolution of the average IS energy per spin $\langle e(t) \rangle$ as function of time. This is obtained by regularly quenching the system down to $T = 0$ to calculate the instantaneous IS energy. The result for a system of $N = 300$ spins and initial temperature $T_i = 3$ is shown in figure 3 (b) for final temperature $T_f = 0.1, 0.2, 0.3$ and 0.4 . The average is over different equilibrium initial configurations at T_i .

The analysis of the figure reveals that the relaxation process can be divided into two different regimes. A first regime independent of T_f , and a second regime independent of both T_i and T_f . The final temperature T_f controls the cross-over between the two regimes. A similar behavior has been observed in molecular dynamics simulations of super-cooled liquids [19]. We note that in our case since we use discrete variables, and hence a faster dynamics, we do not have the very-early regime observed in [19] where $\langle e(t) \rangle$ is almost independent of t .

The two regimes are associated with different relaxation processes. In the first part the system has enough energy and relaxation is mainly due to *path search* out of basins through saddles of energy lower than $k_B T_f$. This part depends only on the initial equilibrium temperature T_i since it sets the initial phase space region. Different T_i leads to different power law. In particular relaxation must slow down as T_i decreases since we expect that lower states are surrounded by higher barriers. This expectation is supported by our numerical data. In figure 4 we report the behavior of $\langle e(t) \rangle$ as function of time for different initial temperatures. The slowing own of the first regime is clearly seen.

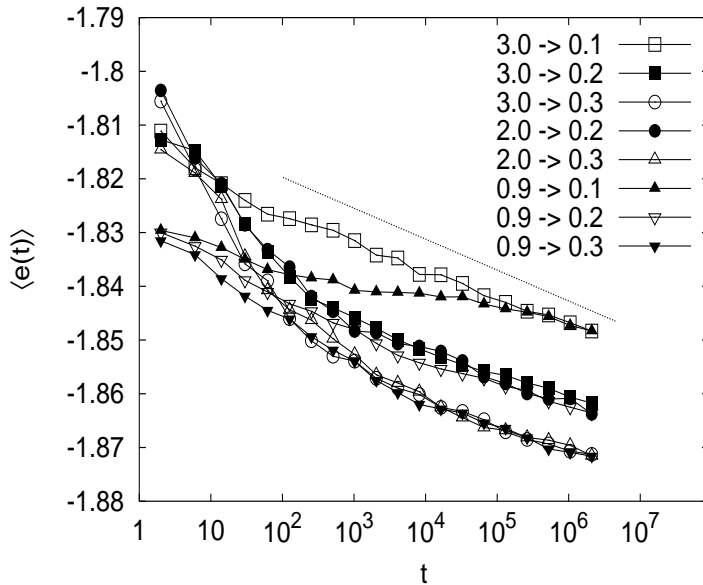


Figure 4. Average inherent structure energy as function of time for initial temperatures $T_i = 3.0, 2.0$ and 0.9 , final temperatures $T_f = 0.1, 0.2$ and 0.3 . The average is over 300 initial configurations. The system size is $N = 300$. The line denotes the slope -0.0025 .

During this process the system explores deeper and deeper valleys (basins) while decreasing its energy. The process stops when all barrier heights become of $O(k_B T_f)$.

From now on the relaxation proceeds only via activated process. A first consequence is that lower the final temperature T_f shorter the first relaxation, in agreement with our findings [See figures 3 and 4].

The analysis of the distance between the instantaneous system state and the corresponding IS, counting the number of single spin flip needed to reach the IS, reveals that for all times the systems stays in configurations few spin flips away from an IS. The number ranging from 8 – 9 for short times to 1 – 2 at larger times. A similar study starting from equilibrium configurations at temperature $T_e(\langle e(t) \rangle)$ evaluated comparing panels (a) and (b) of figure 3 [19] leads to similar numbers. We then conclude that during relaxation the aging system explores the same type of minima (and basins) visited in equilibrium at temperature T_e . Direct consequence is that once the system has reached the activated regime there cannot be memory of the initial T_i , and all curves with different T_i but same T_f should collapse for large time [figure 4].

To have more confidence with this picture of relaxation we have studied the distance from the instantaneous configurations and the nearest saddle to a different basin. This is done by counting the number of spin flips needed to reach the saddle through the *less steep* path, i.e., the path that gives the minimum increase of energy at each spin flip. A typical result is shown in figure 5. Note the strong slowing down at the “kink” where the relaxation law changes.

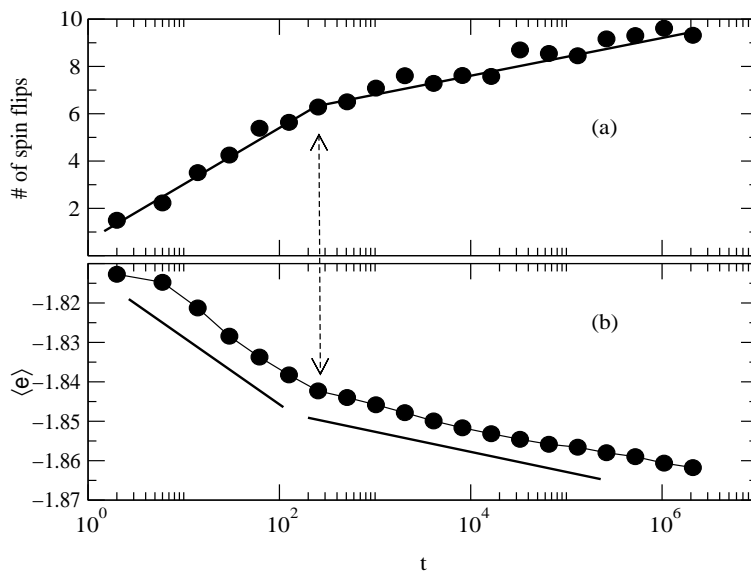


Figure 5. (a) Number of single spin flip to reach the nearest saddle from the IS as a function of t . (b) $\langle e(t) \rangle$ as a function of t during the non-equilibrium process. The system size is $N = 300$, $T_i = 3.0$ and $T_f = 0.2$.

Finally in figure 6 it is shown the average IS energy of IS reached by crossing the saddle nearest to the instantaneous configuration. Note that for short time the crossing leads to IS with similar energies. By comparison we also report the analogous curve obtained starting from the instantaneous IS. In this case the energy is much lower. The picture changes near the kink where both curves merges. Moreover for longer times both curves are above the true relaxation curve, indicating that the

system does not relaxes passing through the *less steep* path. Indeed this is a very special path which may be difficult to find. Higher saddles require higher activation energy but can be found more easily and dominate the relaxation dynamics. More detailed studies of barriers heights and exit time are in progress.

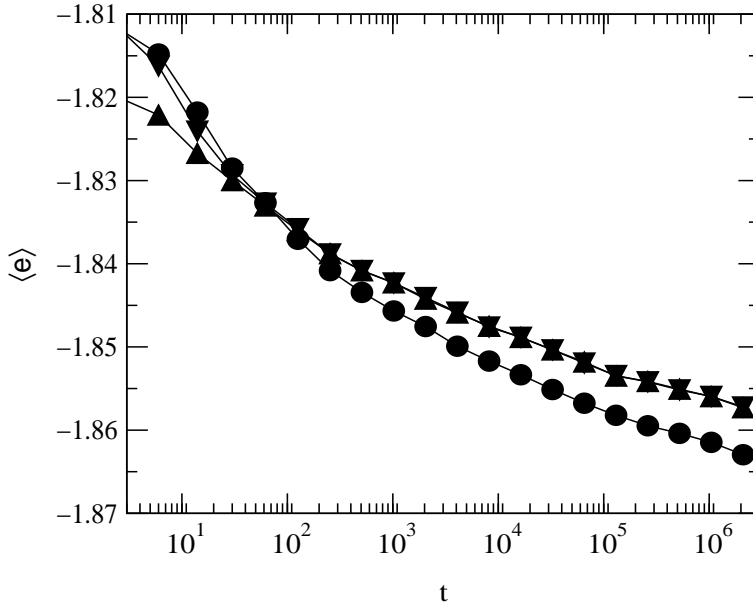


Figure 6. IS energy as function of t for $N = 300$, $T_i = 3.0$ and $T_f = 0.2$. The average is over 300 initial configurations. Symbols are: circle: IS energy from instantaneous configuration; triangle down: IS energy crossing nearest saddle to instantaneous configuration; triangle up: IS energy crossing nearest saddle to instantaneous IS.

3. Conclusions

To summarize, in this work we have shown that *finite-size* mean-field p -spin-like models are good candidates for studying the glass transition. The key point is that near the glass transition the thermodynamics of the systems is dominated by the IS distributions, therefore all systems with similar IS distributions should have similar behavior. Finite-size mean-field p -spin-like models have the double advantage of being analytically tractable for $N \rightarrow \infty$ and easily simulated numerically for finite N , offering good models to analyze the glass transition. Finally we note that the analysis presented in this paper opens the way for the study of generic glass and spin-glass models (such as the Edwards-Anderson model) where a careful study of the thermodynamics associated to the IS has never been considered.

Acknowledgments

We thank for useful discussions C. Donati, U. Marini Bettolo, F. Sciortino and P. Tartaglia.

References

- [1] M. Goldstein, Phys. Rev. **51**, 3728 (1969)
- [2] F. H. Stillinger, Science **267**, 1935 (1995)
- [3] T. B. Schröder, S. Sastry, J. C. Dyre and S. C. Glotzer, cond-mat/9901271
- [4] T. R. Kirkpatrick and D. Thirumalai, Phys. Rev. Lett. **58**, 2091 (1987)
- [5] A. Crisanti, H. Horner and H. J. Sommers, Z. Physik **B92**, 257 (1993)
- [6] A. Crisanti, and H. J. Sommers, Z. Physik **B87**, 341 (1992)
- [7] W. Götze, Z. Physik **B56**, 139 (1984).
- [8] A. Crisanti and H. J. Sommers, J. Phys. I France **5**, 805 (1995)
- [9] A. Crisanti and F. Ritort, cond-mat/9907499
- [10] E. Marinari, G. Parisi and F. Ritort, J. Phys. A (Math. Gen.) **27**, 7847 (1994).
- [11] G. Parisi and M. Potters, J. Phys. A (Math. Gen.) **28**, 5267 (1995)
- [12] T.R. Kirkpatrick and P.G. Wolynes, Phys. Rev. **B36**, 8552 (1987).
- [13] F. H. Stillinger and T. A. Weber, Phys. Rev. **A25**, 978 (1982)
- [14] Strictly speaking there is no T_g for finite systems. We define T_g as the temperature below which the system cannot be equilibrated on the longest Monte Carlo run.
- [15] I. Ohmine, H. Tanaka and P.G. Wolynes, J. Chem Phys. **89**, 5852 (1998); H. Tanaka, Nature **380**, 328 (1996)
- [16] S. Sastry, P.G. Debenedetti and F. H. Stillinger, Nature **393**, 554 (1998)
- [17] F. Sciortino, S. Sastry and P. Tartaglia, cond-mat/9805040
- [18] B. Coluzzi, M. Mezard, G. Parisi and P. Verrocchio, cond-mat/9903129
- [19] W. Kob, F. Sciortino and P. Tartaglia, cond-mat/9905090
- [20] F. Sciortino W. Kob and P. Tartaglia, cond-mat/9906081
- [21] S. Büchner and A. Heuer, cond-mat/9906280
- [22] The intra-basin contribution in liquid is called “vibrational” since it is associated to vibrations near the bottom of the basin.
- [23] F. Sciortino and P. Tartaglia, Phys. Rev. Lett. **78**, 2385 (1997)
- [24] B. Derrida, Phys. Rev. Lett. **45**, 79 (1980)
- [25] A. Crisanti and F. Ritort, in preparation (1999).
- [26] A. J. Bray and M. A. Moore J. Phys. **C14**, 1313 (1981).